Free energy surface of two- and three-dimensional transitions of Au 12 nanoclusters obtained by *ab initio* metadynamics

Gianluca Santarossa,[1] Angelo Vargas,[1,*,†] Marcella Iannuzzi,[2] and Alfons Baiker[1,*,‡]
[1]*Institute for Chemical and Bioengineering, Department of Chemistry and Applied Biosciences, ETH Zurich, Hönggerberg, HCI, 8093 Zurich, Switzerland*
[2]*Institute of Physical Chemistry, University of Zurich, Winterthurerstrasse 190, 8057 Zurich, Switzerland*
(Received 11 February 2010; published 25 May 2010)

The description of the conformational space generated by metal nanoparticles is a fundamental issue for the study of their physicochemical properties. In this investigation, an exhaustive exploration and a unified view of the conformational space of a gold nanocluster is provided using a Au 12 cluster as an example. Such system is characterized by coexisting planar/quasiplanar and tridimensional conformations separated by high-energy barriers. The conformational space of Au 12 has been explored by means of Born-Oppenheimer *ab initio* metadynamics, i.e., a molecular dynamics simulation coupled with a history dependent potential to accelerate events that might occur on a long time scale compared to the time step used in the simulations (rare events). The sampled conformations have complex, in general not intuitive topologies that we have classified as planar/quasiplanar or tridimensional, belonging to different regions of the free energy surface. Three conformational free energy basins were identified, one for the planar/quasiplanar and two for the tridimensional structures. At thermodynamic equilibrium, the planar/quasi-planar and tridimensional conformations were found to coexist, to be fluxional and to be separated by high-free-energy barriers. The comparison between the free energy and the potential energy revealed the relevance of the entropic contribution in the equilibrium distribution of the conformations of the cluster.

DOI: 10.1103/PhysRevB.81.174205 PACS number(s): 61.46.Bc, 61.25.Mv, 61.43.Bn, 61.20.Ja

I. INTRODUCTION

The investigation of metal nanoclusters represents an important multidisciplinary area of research including physics, chemistry, and engineering, with a broad range of possible technological applications.[1–5] An interesting feature of metal nanoclusters consists in the tight relationship between their reactivity and their structural and electronic properties. In this respect, investigating the conformational space generated by metal nanoclusters, i.e., the complete set of shapes that is accessible by such systems, represents a key step for controlling their physicochemical properties and developing new applications. In a recent review, Baletto and Ferrando reported a comprehensive list of the most relevant approaches adopted in the past years.[2] The simplest approach for this kind of investigation consists in collecting topologies based on intuition or on geometrical considerations, thus achieving a sort of experience-driven exploration of the conformational space.[6–11] Due to its nature, this exploration is limited to the study of the simplest geometrical topologies and is not apt to discover more complex, nonobvious conformations. An alternative route is that of following molecular dynamics (MD) trajectories, either at classical[2,12–18] or *ab initio* level.[19–21] In this case the topological features of a cluster are coupled to the dynamic trajectory at a given temperature. Methods such as simulated annealing (SA)[22] can be used to overcome the energy barriers between conformational basins.[23] Other methods aim at the exploration of the conformational space through the application of *ad hoc* algorithms such as Monte Carlo (MC),[24] basin hopping (BH),[25,26] or genetic algorithms (GAs).[27–30] These approaches are commonly known as global optimization methods and have typically been used with classical potentials.[31,32]

Among metal nanoclusters, gold particles in the size range of a few nanometers are particularly interesting, due to their unexpected physicochemical properties. Nanosized Au, for example, is able to catalyze the low-temperature oxidation of CO,[33–35] while bulk gold is known to be inactive.[36] Interesting applications of nanosized gold are also found in nanoelectronics[37–39] and biomedicine.[40–42] For this reason, the structural and electronic properties of gold nanoclusters have been subject of extensive experimental and theoretical investigation in the past years. An exhaustive review on this topic has recently been published by Häkkinen.[43] It is now established that the reactivity of gold nanoclusters is strongly dependent on several factors, including the size, dimensionality, morphology, fluxionality, electronic structure, and charge state of the nanoparticles.[44–67] Numerous indications have been gathered that gold nanoclusters can adopt stable planar, tubular, hollow, or cagelike conformations,[68–78] and it has been proposed that the bias of gold nanoparticles toward planar conformations is due to relativistic effects.[71,79–85]

The study of the conformational free energy surface (FES) of gold nanoparticles below Au 13 is a particularly intriguing example since in this size range the planar structures seem to be more stable than the corresponding cage-like ones.[23,79,81,82,86–94] Trapped ion electron diffraction,[82,90,93,94] photoelectron spectroscopy[86,87] and O_2 titration[96] measurements indicate that the planar/tridimensional transition occurs for $n=12$, i.e., until $n=12$ planar structures seem to be more stable, while for $n>12$ tridimensional structures dominate. Recently, transmission electron microscopy of neutral species have been employed in the reconstruction of the phase map of large gold clusters.[95] These experimental results have been supported by density-functional theory (DFT) calculations including

relativistic effects, as is necessary in order to obtain the order of stability reported by the experiments.[71,79–82] In particular, static calculations using zero order regular approximation (ZORA) (Ref. 97) Hamiltonian combined with the Tao-Perdew-Staroverov-Scuseria (TPSS) (Ref. 98) functional yielded a consistent order of stability between planar and tridimensional conformers.[93] On the other hand, Lechtken *et al.* have shown that also the TPSS functional overestimates the stability of planar clusters.[90] DFT calculations based on generalized gradient approximation (GGA) functionals and with the inclusion of relativistic effects only at the level of the pseudopotential were reported to overestimate the stability of the planar conformations with respect to the tridimensional ones, predicting the planar/tridimensional transition to occur at $n=15$.[93] The coupling between s and d electronic states has been proposed as the bias toward flat structures in gold nanoparticles.[81,82] Koskinen *et al.* suggested that a role could be played by entropic contributions, proposing that GGA-based calculations predict the correct ground state, while experiments could suffer by supercooled metastability of tridimensional conformations.[92] However, the relevance of the entropic contributions addressed in Ref. 92 requires further investigations. *Ab initio* MD simulations of tridimensional gold nanoclusters up to 55 atoms indicate that they consist of fluxional mixtures of tridimensional conformers.[23,91–94] The barriers between tridimensional conformations are easily overcome at room temperature within the time scale of a few ps.[91] On the other hand, although there are indications that planar conformations are relevant, the barriers between the planar and tridimensional conformations are too large to be observed within an affordable simulation time.[23,91,92]

In the present manuscript we will show, using the example of the Au 12 cluster, that an exhaustive description of the conformational space, including both bi- and tridimensional structures, can be achieved by means of a history dependent MD method, known as metadynamics.[99–102] This strategy, accelerating the search for rare events, provides (i) a comprehensive description of the conformational space of the nanocluster, (ii) the reconstruction of the free energy surface of the system as a function of a chosen set of collective variables, (iii) the identification of the conformations belonging to the explored space, (iv) the estimation of the probability of occurrence of each structure, (v) the identification of the transitions between the conformations at room temperature, and (vi) the evaluation of the free energy barriers of interconversion between conformational basins.

II. COMPUTATIONAL METHODS

Metadynamics is a powerful method to accelerate rare events and reconstruct the free energy surface as a function of a set of collective variables σ_α. In its extended Lagrangian formulation, the method is based on the generation of a coarse-grained MD-trajectory in the subspace of the σ_α, by following the evolution of an equal number of auxiliary variables s_α, metadynamics variables. The main assumption is that it is possible to fully describe the processes of interest in terms of the σ_α.[99–102] The extended Lagrangian used to describe the evolution of the system has the form

$$\mathcal{L} = \mathcal{L}_0 + \frac{1}{2}\sum_\alpha M_\alpha s_\alpha^2 - \frac{1}{2}\sum_\alpha k_\alpha[\sigma_\alpha(\mathbf{R}) - s_\alpha]^2 - V(t,\mathbf{s}), \quad (1)$$

where $\mathcal{L}_0$ is the usual Lagrangian of the dynamics, the second term is a fictitious kinetic energy of the s_α, the third term is a restraining term, which correlates the metadynamic variable s_α to the actual value of the collective variable the $\sigma_\alpha(\mathbf{R})$, and $V(t,\mathbf{s})$ is a history dependent potential that force the system to move away from already visited regions of the configurational space. $V(t,\mathbf{s})$ is constructed by superimposing a series of Gaussian beads centered at $\mathbf{s}_i=\{s_\alpha(t_i)\}$ and added at discrete intervals Δt. The resulting time dependent potential has the form

$$V(t,\mathbf{s}) = W\sum_{t_i<t} \exp\left[-\frac{(\mathbf{s}-\mathbf{s}^i)^2}{2\delta\mathbf{s}^2}\right], \quad (2)$$

where W and $\delta\mathbf{s}$ are the height and the width of the Gaussian beads, respectively. With time, the history dependent potential $V(t,\mathbf{s})$ fills the minima of the free energy surface. In the limit of long simulations, the free energy can be reconstructed according to[101,103]

$$\lim_{t\to\infty} V(t,\mathbf{s}) = -\mathcal{F}(\mathbf{s}). \quad (3)$$

In this work, the coordination number (C) and the radius of gyration (R_g) are employed as collective variables. The coordination number $C_{A,B}$ is an average measure of the number of neighbors of type B of the atoms of type A,

$$C_{A,B} = \sum_{i=1}^{N_A}\left[\sum_{\substack{j=1\\ j\neq i}}^{N_B} \frac{1-\left(\frac{r_{ij}}{R_{AB}}\right)^p}{1-\left(\frac{r_{ij}}{R_{AB}}\right)^q}\right], \quad q>p, \quad (4)$$

where N_A and N_B are the number of atoms involved, r_{ij} is the interatomic distance, R_{AB} is the reference distance between A and B, and the exponents p and q determine the decay of the function. In the present case, A and B are both gold atoms and R_{AB} is set equal to 3.4 Å, while p and q are 10 and 16, respectively. Since tridimensional conformations have on average a larger number of neighbors than their planar counterparts, C is larger for tridimensional than for planar conformations. The radius of gyration R_g is a measure of the sphericity of the cluster. R_g is calculated according to

$$R_g^2 = \frac{1}{N}\sum_{i=1}^{N}(r_i-\bar{r})^2, \quad (5)$$

where $\bar{r}$ is the center of mass of the cluster. R_g is closer to unity for tridimensional clusters and becomes larger for planar conformations.

In the current study, the size of the Gaussian beads has been optimized to obtain a trade off between the accuracy of the sampling and an affordable simulation time. W has been set to 4.3×10^{-2} eV, which is in the order of magnitude of the accuracy of the employed Hamiltonian, and allows the comparison of the results with the experimental evidences.

Initial calculations have been run to refine the parameters for the metadynamics simulation, showing that the conformational space generated by the nanocluster in the space of the collective variables is 3×3 a.u.^{2}. The dimension of the external Gaussian potential in the space of the collective variables are ~0.03 a.u. in order to discriminate between different minima on the FES. As a trade off between accuracy and sampling efficiency of the calculation, the values of $\delta\mathbf{s}$ are therefore set to 0.03 for C and 0.03 Å for R_g, resulting in a 100×100 sampling of the conformational space. The Gaussian potential is updated every 50 fs, in order to allow the relaxation of the cluster in between. By comparing the energy and the fluctuations of the metadynamics with the corresponding MD, it has been verified that the physics of the simulation is not influenced by the inclusion of the external potential. Using this setup, 1 ns of simulation was sufficient in order to obtain the final free energy surface.

The metadynamics simulations performed in this investigation are based on DFT as implemented in the CP2K program package, a suite of programs aimed at performing efficient electronic structure calculations and molecular dynamics at different levels of theory.[104] The electronic structure calculations employ the Gaussian and plane wave (GPW) formalism.[105,106] The interaction of the valence electrons with frozen atomic cores is described via the use of norm conserving, dual-space type pseudopotentials.[107] Gold PP includes all the electrons up to the $5p$ levels in the core, thus treating the 11 electrons explicitly in the valence, corresponding to the $5d$ and $6s$ levels. A double-ζ valence plus polarization (DZVP) basis set, optimized according to the Mol-Opt method for the specific Au-PP, has been adopted.[108] For the auxiliary PW expansion of the charge density, the energy cutoff has been set at 180 Ry. The exchange-correlation term was modeled using the Perdew-Burke-Ernzerhof (PBE) functional.[109] Grimme's potential[110,111] has been added in the simulations to include the effects of dispersion forces of gold nanoclusters.[75,79] We found that this setup is optimal for the description of gold bulk, surfaces, and clusters.[91]

All the simulations are performed with periodic boundary conditions, therefore the simulation cells have been chosen large enough (at least 10 Å of vacuum space in all directions) in order to avoid any interaction of the cluster with its periodic images. A time step of 1 fs and a wave function convergence of 10^{-5} guarantee energy conservation for standard MD simulations. The simulation is coupled to a Nose chain of thermostats for keeping the temperature close to the chosen value of 300 K.[112]

The calculations were performed on a CRAY XT5 supercomputer at the Swiss National Computing Center (CSCS) using 48 cores for the run. The number of processors has been chosen as the most effective compromise between calculation efficiency and time consumption. Increasing the number of processors resulted in a consistent performance loss, mostly due to the limited size of the system. 1 ns of simulation took a total of 22 000 cpu hours, corresponding to approximately 1 month of calculations with 48 processors.

Geometry optimizations of selected cluster shapes extracted from the dynamic simulation have been carried out using the Broyden-Fletcher-Goldfarb-Shanno minimization algorithm (BFGS),[113–117] and the structures have been optimized until the atomic displacements were lower than 3×10^{-3} Bohr and the forces lower than 4.5×10^{-4} Ha/Bohr.

III. PRINCIPLES OF METADYNAMICS APPLIED TO A METAL CLUSTER

The current investigation aims at the efficient and accurate sampling of the large conformational space of the Au 12 cluster, focusing on the overall description of the space rather than on the details of a subset of topologies. The complete description of the conformational space of a system requires the calculation of its free energy, which is the combination of enthalpic (dependent on the potential energy) and entropic contributions. The free energy measures the distribution of probability of the available conformers [Eq. (3)], describes completely the thermodynamics of the system under investigation and allows the evaluation of its thermodynamic properties. While the static *ab initio* calculations of a structure, or of a set of structures, return the potential energy surface, and can at best include the contribution from the vibrational states of the system, the free energy also accounts for the total conformational richness coexisting in a given phase, which is of particular importance in the presence of fluxional phases. Within the metadynamics framework, the free energy is reconstructed according to Eq. (3),[102] where the entropic term is directly included in the computation.

The free energy is a function of the total number of degrees of freedom of the system, which, for any nontrivial system, is a large number. However, the topography of the conformational space and the pathways connecting the different basins of attraction can be characterized by one or a few order parameters. The metadynamics approach is based on the identification of these parameters as functions of the degrees of freedom of the system, $\sigma_\alpha(\mathbf{R})$. The trajectory generated by the integration of the equation of motion derived from the extended Lagrangian is projected onto the subspace defined by these parameters, where the probability distribution of the explored regions can be evaluated in terms of time of permanence. The choice of a suitable set of collective variables is a critical issue for the success of the simulation. They should be able to distinguish among the relevant conformers as well as the transition regions. If some important activated process cannot be described in terms of the selected variables, the metadynamics trajectory would hardly explore it. Hence, a poor choice of the collective variables may affect the results by not including possible processes that may contribute significantly to the free energy picture.

In the case under investigation the collective variables should (i) be sensitive to the geometrical properties of the cluster, i.e., the average number of neighbors and the overall geometrical shape of the particle, (ii) sample all of the accessible conformations in the whole space at the given temperature, (iii) explore unexpected structures which would be difficult to sample by other strategies, and (iv) describe the possible pathways connecting the minima on the free energy surface. Previous works have always described Au 12 cluster as a mixture of coexisting conformations with planar and tridimensional topologies, where the tridimensional confor-

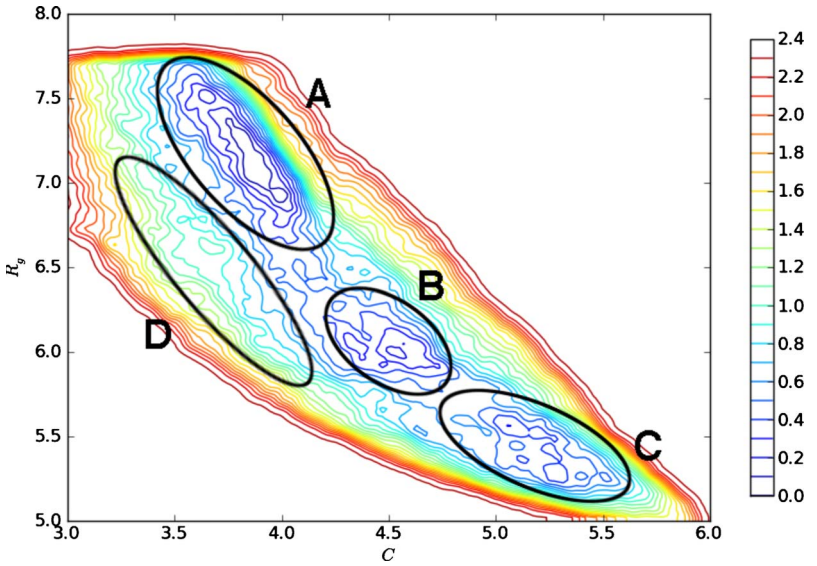

FIG. 1. (Color online) Contour plot of the FES of the conformational space generated by Au 12 as a function of the collective variables C and R_g. The plot shows the free energy differences with respect to the lowest free energy value (eV). The free energy minima are colored in blue (dark gray in the printed version), while the highest free energy values are colored in red (intermediate gray in the printed version).

mations have shapes with cagelike arrangements and no central atoms. In this respect, the coordination number C and the radius of gyration R_g have proven to represent a good set of collective variables. Planar structures have a lower coordination number compared to cagelike ones, since they do not have atomic bonds in the direction of space perpendicular to the plane. On the other hand, cagelike structures have an almost spherical shape, corresponding to $R_g \approx 1$, whereas planar structures are anisotropic, resulting in larger R_g values.

Actually, the metadynamics trajectory has explored a surprisingly large number of unpredicted conformations not belonging either to the planar or to the cagelike group. In other words, the conformational space of Au 12 cluster is mainly populated by tridimensional conformers with complex shapes and nonideal topologies. The perfectly planar and the cagelike conformations represent, indeed, only a minority with respect to the total number of available conformers. These structures are difficult to classify within the common sets established in literature. We show that our choice of collective variables can represent a new description scheme, which is apt to organize the complex identified conformations, thus bridging the gap between the new findings and the former results published in the literature. We could identify four classes that distinguish four regions of the free energy surface reported in Fig. 1. In what follows we refer to these classes as A, B, C, and D. Within this new scheme, each class includes a larger number of conformers, adopting more flexible connotations, if compared to the rigid, although rigorous, topological classification used in the past to sort the conformations.

IV. RESULTS AND DISCUSSION

A. Description of the free energy surface

Figure 1 shows the free energy surface of the conformational space generated by Au 12 at 300 K as a function of C and R_g, reconstructed using the trajectory explored by the metadynamics simulation.[101,102] In the graph of Fig. 1, the z axis reports differences in free energy with respect to a reference point, which has been selected as the point with the lowest free energy. Observing the FES in Fig. 1 we first note the presence of three distinct regions separated by significantly large energy barriers: the first region is characterized by values of C lower than 4.15 and values of R_g greater than 6.5 (region A); the second region corresponds to values of C between 4.15 and 4.75 and values of R_g between 5.7 and 6.5 (region B); the third region is found for values of C greater than 4.75 and values of R_g lower than 5.7 (region C). A fourth region can be isolated at the left side of the FES in Fig. 1, with low values of C and R_g ranging through a large set of values, for which a clear minimum cannot be identified (region D).

In total, within the whole FES, 110 independent, not minima conformers have been isolated. In this context the isolation of a structure means picking a topology from the trajectory of the simulation, with the criterions that: (i) it exists for long enough (a few ps) for not being merely a transition structure, and (ii) it has not been isolated before during the trajectory analysis. The sampling of such a large number of configurations corresponding to independent topologies within a limited amount of time is one of the major achievements of the application of metadynamics. From this point of view, this strategy, coupled with the projection on the potential energy surface, represents a valid approach for solving the global optimization problem. It is important to note that at this point such structures are not optimized. The conformers isolated from the FES are actual, uniquely identified configurations that have been sampled throughout the simulation. In Sec. IV C each one of the isolated structures will be optimized, i.e., projected on the corresponding potential energy surface, thus obtaining minimum energy conformations. The coordinates of the isolated structures and of their minimized conformations are provided in the supplementary material. Within the current study, a detailed discussion of the whole set of conformations is unnecessary. For a clear description of the features of the FES, the most relevant conformers sampled during the simulation are shown in Fig. 2. Region A in Fig. 1 is a deep, long and thin energy well

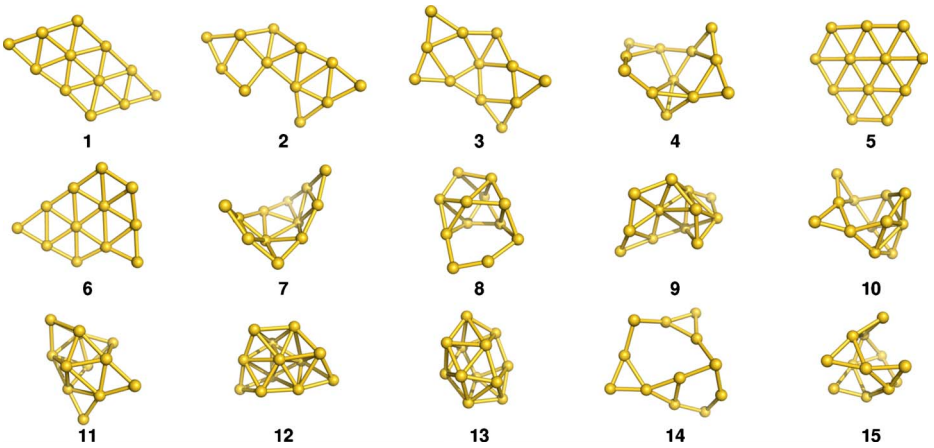

FIG. 2. (Color online) Examples of conformers sampled during the metadynamics simulation. Structures 1–7 belong to region A. Structures 8–11 belong to region B. Structures 12–13 belong to region C. Structures 14–15 belong to region D.

comprising a single minimum, which is characterized by the lowest free energy values. It contains conformations with planar and quasiplanar topologies. During the simulation, 40 different conformers belonging to this region have been identified. A subset of this group is shown in Fig. 2, structures 1–7. The upper part of region A contains conformations characterized by the most anisotropic shapes, with the highest values of R_g, while the lowest part comprises conformations with higher isotropy. Structure 1 of Fig. 2 lays within the deepest area of region A. It has a planar conformation with a rhombic shape, a 4×3 atomic distribution on the plane, and a $\mathcal{C}_{2h}$ symmetry. Most of the conformations found in region A, such as structure 2 of Fig. 2, are perturbations of the topology of structure 1. Other conformers belonging to region A have scaffolds similar to structure 1, with the displacement of several atoms either in plane (structure 3) or out of the plane (structure 4). The effect of these atomic displacements is that of lowering the symmetry of the conformations. Note that structures 1 to 4 can interconvert via minimal in-plane or out-of-plane displacements of the constituting atoms. In the lowest part of region A the isolated conformations have either large in-plane isotropy (structure 5), in-plane displacements of a few atoms (structure 6), or bended planar structures (structure 7). Structure 5, in particular, is very interesting, due to its planar topology, the high $\mathcal{D}_{3h}$ symmetry, and the favorable enthalpy (minimum 1 of Table II), which will be discussed in the section about the potential energy. Region A is therefore a mixture of several conformations, having similar free energies, and topologically characterized by different levels of perturbations of the main structure (structure 1).

Regions B and C contain tridimensional structures, including the cagelike conformations. 50 different conformers could be identified, examples of which are reported in Fig. 2, structures 8–13. Region B is a small basin with a single minimum, which lays at ~0.25 eV higher free energy compared to region A and is ~0.3 eV deep. Topologies in region B are elongated and anisotropic, and may have a set of low-coordinated atoms (structure 8). There are examples of widely open structures (structure 9), tridimensional clusters with a flat appendix (structure 10) or completely compact structures (structure 11). Region C is extended through a consistently large area in the free energy space at 0.4 eV higher free energy than region A, with several small minima at just 0.25 eV higher energy than the free energy minimum. Region C contains spherelike conformations with large coordination numbers. The cagelike conformers known in the literature map in this region. In this area the clusters have compact structures with widely varying shapes (structures 12–13).

Besides minima A, B, and C, there is a large shallow area at higher free energy (region D). This area is characterized by not having local minima, i.e., it is not corrugated. Region D lays at ~0.8–1.0 eV higher free energy than region A, and it extends through a large area on the FES. In region D, 20 different conformers have been identified. Figure 2 shows two representative conformations belonging to this area (structures 14–15). Interesting conformations belong to this region. In general, the topologies found in region D are characterized by stretched conformations with lower number of bonds, longer bond lengths and ring-like arrangements of the atoms, which do not properly belong either to the planar/quasi-planar or to the cage-like structures (structures 14–15). The conformations in region D are essential to completely explore the conformational space. In fact, from the free energy profile it is possible to estimate the fraction of planar/quasiplanar and tridimensional conformations that are expected to be simultaneously present at thermodynamic equilibrium, i.e., an estimate of the frequency of occurrence of each set of conformations at any given time. This information is obtained by integrating the free energy in the space of the collective variables for each of the regions A, B, C, and D. The results are reported in Table I and show that conformations in basin D add up to almost 30% of the total

TABLE I. Probability distribution of regions A-D on the FES.

Basin	A	B	C	D	planar/quasiplanar	Tridimensional
Frequency (%)	31	22	18	29	48	52

TABLE II. Potential energy differences (eV) of the 57 optimized geometries obtained from the selected conformers on the metadynamics trajectory (see text). The differences are calculated with respect to the absolute minimum energy found for minimum 1. The corresponding structures are shown in Figures S1 and S2 in Ref. 118.

Id	1	2	3	4	5	6	7	8	9	10
ΔE	0.00	0.28	0.40	0.56	0.65	0.65	0.78	0.89	0.89	1.00
Id	11	12	13	14	15	16	17	18	19	20
ΔE	1.64	1.64	0.46	0.52	0.53	0.53	0.56	0.57	0.58	0.60
Id	21	22	23	24	25	26	27	28	29	30
ΔE	0.61	0.61	0.61	0.67	0.70	0.70	0.75	0.78	0.79	1.02
Id	31	32	33	34	35	36	37	38	39	40
ΔE	0.29	0.39	0.40	0.46	0.46	0.47	0.49	0.54	0.54	0.55
Id	41	42	43	44	45	46	47	48	49	50
ΔE	0.58	0.65	0.67	1.06	0.61	0.63	0.39	0.48	0.54	0.56
Id	51	52	53	54	55	56	57			
ΔE	0.58	0.62	0.62	0.65	1.01	1.09	1.47			

conformational space. The planar/quasi-planar subspace defined in Table I has R_g values larger than 6.5, and comprises both region A and a part of region D. The tridimensional subspace has R_g values lower than 6.5 and comprise regions B, C, and part of D. The results of Table I show that the planar/quasi-planar and the tridimensional conformations appear for approximately 48% and 52% of the total, respectively. At room temperature both the planar/quasi-planar structures, containing the planar conformers, and the tridimensional conformations, containing the cagelike conformers, are present at equilibrium with comparable frequencies, consistently with the experiments.[82,86,87,90,93,94] These results indicate that DFT calculations with GGA functionals are sufficiently accurate to describe the experimental findings, if the entropic contributions are taken into account. This claim is not in contradiction with the results of Johansson *et al.*, which are based on static calculations with TPSS functional. New generation functionals such as TPSS may be applied to MD or metadynamics simulations in the future in order to further improve the accuracy of the simulation, although the increase in the computational cost will not be negligible. The tridimensional conformers with cagelike shapes (region C) account for less than half of the total number of tridimensional conformers. Therefore the conformations belonging to regions B and D, although characterized by nonintuitive irregular shapes, are of fundamental importance for the complete description of the tridimensional space.

B. Description of the activation free energy

Having access to the complete conformational FES also allows the estimation of the activation free energies for the process of conversion between structures. An evaluation of the activation free energy can simply be obtained by calculating the difference in free energy between the bottom of the basin and the transition region. The energy barrier separating region A from region B is ~0.55 eV. The barrier separating region B from region A is ~0.3 eV high. The energy barriers between region B and region C are of ~0.4 eV on both sides. At 300 K, such energy barriers are larger than k_BT (which is in the order of magnitude of 0.03 eV). Therefore, at room temperature the interconversions between planar/quasi-planar and tridimensional conformations are rare events, and they occur at time scales that are not affordable by current *ab initio* molecular dynamics. This is consistent with the results obtained from MD simulations at 300 K on Au 12, which showed that within tens of picoseconds cagelike structures do not interconvert with planar conformations.[91] This observation emphasizes the importance of the application of enhanced schemes such as metadynamics to explore the conformational space of small metal clusters.

On the contrary, the interconversions between conformations occurring within region A take place without overcoming any significant activation barrier. Region B shows the same features of region A, where no activation barriers could be identified, and the clusters can interconvert rapidly to one another. Region C is more complex to describe, but within the different basins several topologies interconvert within the time scale of the picoseconds. This continuous interchange between conformations at room temperature is the main characteristic of fluxional behavior.[91] Structures within these basins are therefore fluxional, being characterized by the low temperature interconversion of numerous different topological arrangements of the nuclei. These findings confirm the presence of planar fluxional phases described in the investigation of Ref. 92.

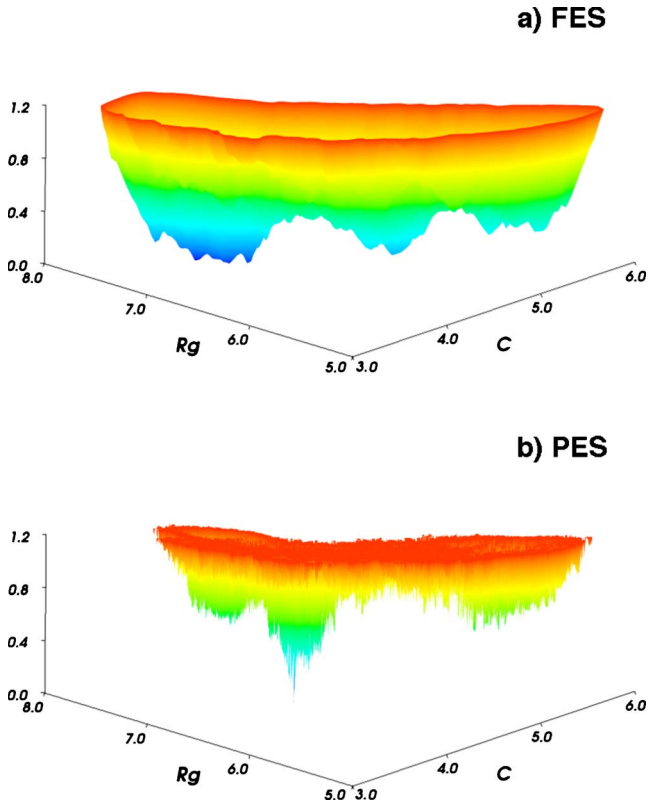

FIG. 3. (Color online) Comparison between the FES (a) and the PES (b) generated by Au 12 as a function of the collective variables C and R_g. The plot shows the free energy differences with respect to the lowest free energy value (eV). The free energy minima are colored in blue (dark gray in the printed version), while the highest free energy values are colored in red (intermediate gray in the printed version). The conformation depicted in the picture corresponds to minimum 1.

C. Relationship between the FES and the PES

In the past years several static calculations have been reported unveiling a large amount of informations about the range of stability of Au clusters at 0 K.[79,81,82,86–90] The study of the free energy surface performed in the current investigation, on the other hand, constitutes a new strategy providing information that are complementary to static calculations. It is therefore relevant to compare the results of the current investigation with those reported in previous works.

Figure 3 shows the comparison between (a) the FES and (b) the PES of the Au 12 nanoparticle obtained through the metadynamics simulation. The study of the FES of the Au 12 cluster has shown that at room temperature this cluster consists of a mixture of complex tridimensional conformations, within which planar and cage-like conformers represent only a subset. Four classes of conformations with comparable probability of occurrence could be isolated. These correspond to four basins on the FES, separated by relatively high-conversion barriers. The tridimensional conformations are only moderately more frequently observed than the planar/quasiplanar counterparts, mostly due to the larger number of possible tridimensional atomic arrangements, resulting in a larger statistical weight, i.e., larger conformational entropy.

As shown in Fig. 3, the PES is significantly different from the FES. On the potential energy surface [Fig. 3(b)], only three minima could be clearly identified, two of which overlap with basin A on the FES, and one with basin C. Of the two minima corresponding to basin A, one consists in a dominant, deep and narrow basin containing a single global minimum topology. The conformation corresponding to the global minimum is structure 5 shown in Fig. 2, and named minimum 1 in Table II. The second region corresponding to basin A, located at lower C and higher R_g, is ~0.3–0.6 eV higher in energy compared to minimum 1. Tridimensional conformations of regions B and C lay at ~0.6–0.85 eV higher potential energy compared to minimum 1. On the PES, the conformations of region D lay at even higher energy and are therefore largely enthalpically unfavored.

The study of the PES confirms that planar structures are indeed enthalpically more stable than all the other conformers, with the presence of an unique conformation strikingly more stable than all the others. On the other hand, on the FES several conformers with different potential energies possess comparable free energies. The existence of conformations with different potential energies but similar free energies marks a clear distinction between the potential energy and the free energy of the system and pinpoints the role of entropy in characterizing favorable atomic arrangements. In other words, if considering only the potential energy (static calculations at 0 K), minimum 1 would result by far the most stable. Having this information alone would lead to the conclusion that minimum 1 should be the only conformation present at equilibrium. On the contrary, the study of the FES shows that basin A is characterized by the presence of several different topologies, which at room temperature easily interconvert.

With the aim of further characterizing the features of the PES, the potential energy minima of Au 12 cluster have been explored, through geometry optimization of the conformations isolated on the FES. Hence, the 110 conformations selected from the metadynamics trajectory and discussed in Sec. IV A are projected on the PES by structural optimization, thus isolating 57 different minima. Among them, some have already been reported in the literature,[79,81,82,86–90] but many are encountered here for the first time. The isolated minima on the PES are fewer than the initial number of conformers that have been optimized. This indicates that more temporary structures explored at finite temperature belong to the same basin of attraction on the PES. The potential energy of the isolated conformers are reported in Table II, where the reference structure corresponding to the absolute minimum energy (minimum 1) is structure 5 of Fig. 2. The corresponding topologies are shown in Figures S1 and S2 in Ref. 118.

The optimization of conformations belonging to region A leads to 12 independent minima (Figure S1, structures 1–12), from regions B and C 32 tridimensional minima have been found (Figure S1, structures 13–30 and Figure S2, structures 31–44), and 13 conformers were isolated from region D (Figure S2, structures 45–57). Some conformations of region D fall, after optimization, to structures belonging to one of the other regions, confirming the transition character of this portion of the conformational space. As shown in Table II,

minimum 1 is the most stable conformer on the PES. All the others report energies between. 0.3 eV and 1.5 eV higher. The potential energy of the isolated conformations within the whole PES largely varies with the topology. Within the class of planar/quasi-planar structures, the different minima present quite large energy variations, with a maximal energy difference of 1.64 eV. The potential energies of tridimensional conformations vary typically within smaller ranges (max. ΔE_B=0.56 eV, max. ΔE_C=0.77 eV, and max. ΔE_D =0.86 eV) and on average are less stable than the lowest planar minima. The potential energies of the conformers belonging to region D are on average the highest. The large variety of structures and energies makes it difficult to rationalize the elements that lead to stability. Symmetry, number of highly coordinated atoms, bond distances, seem all to play a role in the stabilization of the structure, but in a convoluted manner. New structural descriptors able to determine more accurate topology-stability relationships might be useful to provide further informations on the reaction pathways and reactivity of the system.

V. CONCLUSIONS

In this investigation, *ab initio* metadynamics has been applied using the coordination number C and the radius of gyration R_g as collective variables to explore conformational space of a Au 12 cluster. The FES of the system has been reconstructed as a function of the selected collective variables. Au 12 represents an interesting case of study due to its complexity since both planar/quasiplanar and tridimensional conformations have been shown to coexist at thermodynamic equilibrium. A large portion of the conformational space has been sampled by the simulation, revealing an unexpected conformational richness consisting of a combination of planar/quasiplanar and tridimensional structures. 110 highly probable conformations have been identified on the FES, from which 57 structures have been isolated as minima on the PES. The tridimensional conformations are shown to be slightly more frequent than the planar conformations due to their favorable conformational entropy.

The FES of the Au 12 cluster provides a thermodynamically exhaustive description of the conformational space of the nanoparticle by correctly accounting for the enthalpic and the entropic terms characterizing the system. Since the entropy plays a relevant role, the reconstruction of the PES alone turns out to be inadequate to correctly describe the properties of a fluxional system. This is the case of Au 12 nanocluster, where the entropic contribution is essential to correctly evaluate the probability of exploring different regions of the conformational space. The activation energies of the most significant interconversions have been analyzed, confirming the fluxional behavior at room temperature within both the planar/quasi-planar and the tridimensional regions. High activation barriers have been recorded, instead, for the interconversions between different classes. The application of metadynamics, which allows the thorough exploration of the conformational space of the system within a long, but affordable simulation time, has provided a consistent picture of the relation between topology and free energy for a metal cluster. Several high energy conformations have been disclosed that would have otherwise been difficult to identify, even if they represent a consistent fraction of the accessible FES. Providing access to such conformations could prove useful for the study of reactivity, since this set of conformers could be a valid trade-off between stability and accessibility to reaction sites.

This study concurs to the unification of a classical thermodynamic description of the investigated system to the quantum mechanical treatment of the atomic model. This strategy provides evidence that the distribution of conformers in nanoparticles has a consistent entropic contribution. While the use of static calculations on the single conformers might give only partial insights into the problem, the exploration of free energy landscapes provides a much broader picture and relevantly contributes to the rationalization of the properties of nanoclusters.

ACKNOWLEDGMENTS

Financial support from the Swiss National Science Foundation is kindly acknowledged. The Swiss National Supercomputing Centre (CSCS, Manno) and ETHZ are acknowledged for providing computing resources.

*Corresponding author.
†vargas@chem.ethz.ch
‡baiker@chem.ethz.ch

[1] J. P. Wilcoxon and B. L. Abrams, Chem. Soc. Rev. **35**, 1162 (2006).
[2] F. Baletto and R. Ferrando, Rev. Mod. Phys. **77**, 371 (2005).
[3] C. Burda, X. Chen, R. Narayanan, and M. El-Sayed, Chem. Rev. (Washington, D.C.) **105**, 1025 (2005).
[4] D. L. Feldheim and C. A. Foss, Jr., *Metal Nanoparticles: Synthesis, Characterization and Applications* (CRC Press, Boca Raton, FL/Taylor & Francis Group, London, 2002).
[5] T. Schalkhammer, Monatsch. Chem. **129**, 1067 (1998).
[6] F. Viñes, F. Illas, and K. M. Neyman, J. Phys. Chem. A **112**, 8911 (2008).
[7] Q. Ge, C. Song, and L. Wang, Comput. Mater. Sci. **35**, 247 (2006).
[8] C. Song, Q. Ge, and L. Wang, J. Phys. Chem. B **109**, 22341 (2005).
[9] T. Pawluk, Y. Hirata, and L. Wang, J. Phys. Chem. B **109**, 20817 (2005).
[10] L. Xiao and L. Wang, Chem. Phys. Lett. **392**, 452 (2004).
[11] L. Xiao and L. Wang, J. Phys. Chem. A **108**, 8605 (2004).
[12] N. E. Schultz, A. W. Jasper, D. Bhatt, J. I. Siepmann, and D. G. Truhlar, *Multiscale Simulation Methods for Nanomaterials* (Wiley, New York, 2008).
[13] S. Alkis, J. L. Krause, J. N. Fry, and H. P. Cheng, Phys. Rev. B

79, 121402(R) (2009).
[14] D. H. Seo, H. Y. Kim, J. H. Ryu, and H. M. Lee, J. Phys. Chem. C **113**, 10416 (2009).
[15] I. F. Golovnev, E. I. Golovneva, and V. M. Fomin, Phys. Mesomech. **11**, 19 (2008).
[16] A. Moitra, S. Kim, J. Houze, B. Jelinek, S.-G. Kim, S.-J. Park, R. M. German, and M. F. Horstemeyer, J. Phys. D **41**, 185406 (2008).
[17] I. Baranov *et al.*, Nucl. Instrum. Methods Phys. Res. B **266**, 1993 (2008).
[18] S. K. R. S. Sankaranarayanan, V. R. Bhethanabotla, and B. Joseph, J. Phys. Chem. C **111**, 2430 (2007).
[19] M. Iannuzzi, *Computational Methods in Catalysis and Materials Science* (Wiley-VCH Verlag GmbH & Co, KGaA, Weinheim, 2009).
[20] D. Marx and J. Hutter, *Modern Methods and Algorithms of Quantum Chemistry* (John von Neumann Institute for Computing, Forschungszentrum Jülich, 2000), pp. 301–449.
[21] C. Yannouleas, U. Landman, and R. Barnett, *Metal Clusters* (Wiley, New York, 1999), pp. 145–180.
[22] L. Wille, Comput. Mater. Sci. **17**, 551 (2000).
[23] C. H. Hu, C. Chizallet, H. Toulhoat, and P. Raybaud, Phys. Rev. B **79**, 195416 (2009).
[24] N. Metropolis and S. Ulam, J. Am. Stat. Assoc. **44**, 335 (1949).
[25] D. Wales and H. Scheraga, Science **285**, 1368 (1999).
[26] D. Wales and J. Doye, J. Phys. Chem. A **101**, 5111 (1997).
[27] R. L. Johnston, Dalton Trans. **2003**, 4193.
[28] I. Garzon, M. Beltran, G. Gonzalez, I. Gutierrez-Gonzalez, K. Michaelian, J. Reyes-Nava, and J. Rodriguez-Hernandez, Eur. Phys. J. D **24**, 105 (2003).
[29] M. Wolf and U. Landman, J. Phys. Chem. A **102**, 6129 (1998).
[30] M. Mitchell, *An Introduction to Genetic Algorithms* (MIT Press, Cambridge, MA, 1996).
[31] X. Shao, X. Yang, and W. Cai, J. Comput. Chem. **29**, 1772 (2008).
[32] T. J. Toai, G. Rossi, and R. Ferrando, Faraday Discuss. **138**, 49 (2008).
[33] G. Bond and D. Thompson, Gold Bull. **33**, 41 (2000).
[34] M. Haruta, N. Yamada, T. Kobayashi, and S. Iijima, J. Catal. **115**, 301 (1989).
[35] M. Haruta, T. Kobayashi, H. Sano, and N. Yamada, Chem. Lett. **16**, 405 (1987).
[36] B. Hammer and J. K. Nørskov, Nature (London) **376**, 238 (1995).
[37] C. R. Martin and P. Kohli, Nat. Rev. Drug Discovery **2**, 29 (2003).
[38] A. Tkachenko, H. Xie, D. Coleman, W. Glomm, J. Ryan, M. Anderson, S. Franzen, and D. Feldheim, J. Am. Chem. Soc. **125**, 4700 (2003).
[39] Q. Wang, T. Lin, L. Tang, J. Johnson, and M. Finn, Angew. Chem., Int. Ed. **41**, 459 (2002).
[40] M. Tsoli, H. Kuhn, W. Brandau, H. Esche, and G. Schmid, Small **1**, 841 (2005).
[41] M.-C. Daniel and D. Astruc, Chem. Rev. (Washington, D.C.) **104**, 293 (2004).
[42] H. Zhang, G. Schmid, and U. Hartmann, Nano Lett. **3**, 305 (2003).
[43] H. Häkkinen, Chem. Soc. Rev. **37**, 1847 (2008).
[44] X. Zhou, W. Xu, G. Liu, D. Panda, and P. Chen, J. Am. Chem. Soc. **132**, 138 (2010).
[45] G. Shafai, S. Hong, M. Bertino, and T. S. Rahman, J. Phys. Chem. C **113**, 12072 (2009).
[46] A. Prestianni, A. Martorana, F. Labat, I. Ciofini, and C. Adamo, J. Mol. Struct.: THEOCHEM **903**, 34 (2009).
[47] S. M. Lang, T. M. Bernhardt, R. N. Barnett, B. Yoon, and U. Landman, J. Am. Chem. Soc. **131**, 8939 (2009).
[48] C. Harding, V. Habibpour, S. Kunz, A. N.-S. Farnbacher, U. Heiz, B. Yoon, and U. Landman, J. Am. Chem. Soc. **131**, 538 (2009).
[49] G. M. Veith, A. R. Lupini, S. Rashkeev, S. J. Pennycook, D. R. Mullins, V. Schwartz, C. A. Bridges, and N. J. Dudney, J. Catal. **262**, 92 (2009).
[50] M. B. Torres, E. M. Fernandez, and L. C. Balbas, J. Phys. Chem. A **112**, 6678 (2008).
[51] K. P. McKenna, P. V. Sushko, and A. L. Shluger, J. Chem. Phys. **126**, 154704 (2007).
[52] K. P. McKenna, P. V. Sushko, and A. L. Shluger, J. Phys. Chem. C **111**, 2823 (2007).
[53] K. P. McKenna and A. Shluger, J. Phys. Chem. C **111**, 18848 (2007).
[54] J. A. van Bokhoven and J. T. Miller, J. Phys. Chem. C **111**, 9245 (2007).
[55] U. Landman, B. Yoon, C. Zhang, U. Heiz, and M. Arenz, Top. Catal. **44**, 145 (2007).
[56] C. Zhang, B. Yoon, and U. Landman, J. Am. Chem. Soc. **129**, 2228 (2007).
[57] B. Yoon, P. Koskinen, B. Huber, O. Kostko, B. von Issendorff, H. Häkkinen, M. Moseler, and U. Landman, ChemPhysChem **8**, 157 (2007).
[58] M. Arenz, U. Landman, and U. Heiz, ChemPhysChem **7**, 1871 (2006).
[59] M. Walter and H. Häkkinen, Phys. Chem. Chem. Phys. **8**, 5407 (2006).
[60] B. Yoon, H. Häkkinen, U. Landman, A. Worz, J. Antonietti, S. Abbet, K. Judai, and U. Heiz, Science **307**, 403 (2005).
[61] I. N. Remediakis, N. Lopez, and J. K. Nørskov, Appl. Catal., A **291**, 13 (2005).
[62] L. M. Molina and B. Hammer, Appl. Catal., A **291**, 21 (2005).
[63] C. T. Campbell, Science **306**, 234 (2004).
[64] H. Häkkinen, S. Abbet, A. Sanchez, U. Heiz, and U. Landman, Angew. Chem., Int. Ed. **42**, 1297 (2003).
[65] B. Yoon, H. Häkkinen, and U. Landman, J. Phys. Chem. A **107**, 4066 (2003).
[66] G. Mills, M. Gordon, and H. Metiu, J. Chem. Phys. **118**, 4198 (2003).
[67] A. Sanchez, S. Abbet, U. Heiz, W. Schneider, H. Häkkinen, R. Barnett, and U. Landman, J. Phys. Chem. A **103**, 9573 (1999).
[68] Z. Y. Li, N. P. Young, M. D. Vece, S. Palomba, R. E. Palmer, A. L. Bleloch, B. C. Curley, R. L. Johnston, J. Jiang, and J. Yuan, Nature (London) **451**, 46 (2008).
[69] D. Tian and J. Zhao, J. Phys. Chem. A **112**, 3141 (2008).
[70] J. Wang, H. Ning, Q.-M. Ma, Y. Liu, and Y.-C. Li, J. Chem. Phys. **129**, 134705 (2008).
[71] W. Huang, M. Ji, C.-D. Dong, X. Gu, L.-M. Wang, X. G. Gong, and L.-S. Wang, ACS Nano **2**, 897 (2008).
[72] A. J. Karttunen, M. Linnolahti, T. A. Pakkanen, and P. Pyykkö, Chem. Commun. (Cambridge) **2008**, 465.
[73] D. Tian, J. Zhao, B. Wang, and R. B. King, J. Phys. Chem. A **111**, 411 (2007).
[74] A. Lechtken, D. Schooss, J. R. Stairs, M. N. Blom, F. Furche, N.

Morgner, O. Kostko, B. von Issendorff, and M. M. Kappes, Angew. Chem., Int. Ed. **46**, 2944 (2007).
[75] X. Gu, S. Bulusu, X. Li, X. C. Zeng, J. Li, X. G. Gong, and L.-S. Wang, J. Phys. Chem. C **111**, 8228 (2007).
[76] L. Xiao, B. Tollberg, X. Hu, and L. Wang, J. Chem. Phys. **124**, 114309 (2006).
[77] M. P. Johansson, D. Sundholm, and J. Vaara, Angew. Chem., Int. Ed. **43**, 2678 (2004).
[78] X. Gu, M. Ji, S. H. Wei, and X. G. Gong, Phys. Rev. B **70**, 205401 (2004).
[79] E. M. Fernandez, J. M. Soler, and L. C. Balbas, Phys. Rev. B **73**, 235433 (2006).
[80] H. Häkkinen, M. Moseler, O. Kostko, N. Morgner, M. A. Hoffmann, and B. v. Issendorff, Phys. Rev. Lett. **93**, 093401 (2004).
[81] H. Häkkinen, M. Moseler, and U. Landman, Phys. Rev. Lett. **89**, 033401 (2002).
[82] F. Furche, R. Ahlrichs, P. Weis, C. Jacob, S. Gilb, T. Bierweiler, and M. Kappes, J. Chem. Phys. **117**, 6982 (2002).
[83] P. Pyykko, Inorg. Chim. Acta **358**, 4113 (2005).
[84] P. Pyykko, Angew. Chem., Int. Ed. **43**, 4412 (2004).
[85] P. Pyykko, Chem. Rev. (Washington, D.C.) **88**, 563 (1988).
[86] P. Gruene, D. M. Rayner, B. Redlich, A. F. G. van der Meer, J. T. Lyon, G. Meijer, and A. Fielicke, Science **321**, 674 (2008).
[87] S. Bulusu, X. Li, L.-S. Wang, and X. C. Zeng, Proc. Natl. Acad. Sci. U.S.A. **103**, 8326 (2006).
[88] E. Apra, R. Ferrando, and A. Fortunelli, Phys. Rev. B **73**, 205414 (2006).
[89] J. Li, X. Li, H. Zhai, and L. Wang, Science **299**, 864 (2003).
[90] A. Lechtken, C. Neiss, M. M. Kappes, and D. Schooss, Phys. Chem. Chem. Phys. **11**, 4344 (2009).
[91] A. Vargas, G. Santarossa, M. Iannuzzi, and A. Baiker, Phys. Rev. B **80**, 195421 (2009).
[92] P. Koskinen, H. Häkkinen, B. Huber, B. von Issendorff, and M. Moseler, Phys. Rev. Lett. **98**, 015701 (2007).
[93] M. P. Johansson, A. Lechtken, D. Schooss, M. M. Kappes, and F. Furche, Phys. Rev. A **77**, 053202 (2008).
[94] X. Xing, B. Yoon, U. Landman, and J. H. Parks, Phys. Rev. B **74**, 165423 (2006).
[95] A. S. Barnard, N. P. Young, A. I. Kirkland, M. A. van Huis, and H. Xu, ACS Nano **3**, 1431 (2009).
[96] W. Huang, S. Bulusu, R. Pal, X. C. Zeng, and L.-S. Wang, ACS Nano **3**, 1225 (2009).
[97] E. van Lenthe, E. J. Baerends, and J. Snijders, J. Chem. Phys. **99**, 4597 (1993).
[98] J. Tao, J. P. Perdew, V. N. Staroverov, and G. E. Scuseria, Phys. Rev. Lett. **91**, 146401 (2003).
[99] A. Laio and F. L. Gervasio, Rep. Prog. Phys. **71**, 126601 (2008).
[100] A. Laio and M. Parrinello, Lect. Notes Phys. **703**, 315 (2006).
[101] M. Iannuzzi, A. Laio, and M. Parrinello, Phys. Rev. Lett. **90**, 238302 (2003).
[102] A. Laio and M. Parrinello, Proc. Natl. Acad. Sci. U.S.A. **99**, 12562 (2002).
[103] C. Micheletti, A. Laio, and M. Parrinello, Phys. Rev. Lett. **92**, 170601 (2004).
[104] J. VandeVondele, M. Krack, F. Mohamed, M. Parrinello, T. Chassaing, and J. Hutter, Comput. Phys. Commun. **167**, 103 (2005).
[105] G. Lippert, J. Hutter, and M. Parrinello, Theor. Chem. Acc. **103**, 124 (1999).
[106] G. Lippert, J. Hutter, and M. Parrinello, Mol. Phys. **92**, 477 (1997).
[107] S. Goedecker, M. Teter, and J. Hutter, Phys. Rev. B **54**, 1703 (1996).
[108] J. VandeVondele and J. Hutter, J. Chem. Phys. **127**, 114105 (2007).
[109] J. P. Perdew, K. Burke, and M. Ernzerhof, Phys. Rev. Lett. **77**, 3865 (1996).
[110] S. Grimme, J. Comput. Chem. **27**, 1787 (2006).
[111] S. Grimme, J. Comput. Chem. **25**, 1463 (2004).
[112] S. Nose, J. Chem. Phys. **81**, 511 (1984).
[113] C. Broyden, Math. Comput. **24**, 365 (1970).
[114] J. Nocedal, Math. Comput. **35**, 773 (1980).
[115] D. Liu and J. Nocedal, SIAM (Soc. Ind. Appl. Math.) J. Sci. Stat. Comput. **10**, 1 (1989).
[116] D. Shanno and P. Kettler, Math. Comput. **24**, 657 (1970).
[117] D. Goldfarb, Math. Comput. **24**, 23 (1970).
[118] See supplementary material at http://link.aps.org/supplemental/10.1103/PhysRevB.81.174205 for Figures S1 and S2 showing the conformations of the minima isolated on the PES, for the complete set of coordinates of the conformations isolated on the FES, and for their projections on the PES.